ELSEVIER

Journal of Molecular Catalysis A: Chemical 112 (1996) 43–54

JOURNAL OF MOLECULAR CATALYSIS A: CHEMICAL

Highly selective vapor phase propene hydroformylation catalyzed by Rh/B and Rh–Co/B systems on silica

Loretta Storaro [a], Renzo Ganzerla [a], Maurizio Lenarda [a,*], Roberto Zanoni [b], Guido Righini [c]

[a] *Dipartimento di Chimica, Università di Venezia, D.D. 2137, 30123 Venice, Italy*
[b] *Dipartimento di Chimica, Università di Roma (La Sapienza), Piazzale A. Moro 5, 00185 Rome, Italy*
[c] *ICMAT-CNR, 00016, Monterotondo Stazione, Roma, Italy*

Received 6 March 1996; accepted 18 June 1996

Abstract

The reduction of cobalt and rhodium salts coadsorbed on silica by aqueous $NaBH_4$ at 273 K in Ar allows the synthesis of catalytic systems formed by very small rhodium crystallites (< 4 nm) and cobalt oxide/hydroxide. The presence of an unreduced cobalt species is well documented by TPR and XPS. The cobalt oxide is probably deposited on the rhodium surface, obscuring a large amount of the active metal centers. As can be judged by FT-IR and XRD data the morphology of the system is not modified by thermal treatments in CO and H_2. The system resulted inactive for the atmospheric hydroformylation of propene, but actively catalyzed the reaction when a slight pressure (506 kPa) was applied. The high values of chemoselectivity towards hydroformylation ($R = 0.75$) and regioselectivity to linear aldehydes ($S_L = 96$) can be due to the electronic and steric effects of the cobalt oxide layer.

Keywords: Silica; Propene; Hydroformylation; Rhodium; Cobalt; Boron

1. Introduction

Rhodium based systems, supported on various inorganic carriers are the most studied heterogeneous catalysts for the atmospheric vapor phase hydroformylation of light olefins [1–40]. However, monometallic rhodium catalysts have low overall activity and low chemoselectivity towards hydroformylation. Higher activity and an improved chemoselectivity in vapor phase were obtained by doping the catalyst surface with S [13,18,26,30,31] or Se [16,27,28], adding promoters such as alkaly [19,25,39,40] or Zn cations [10,11] or using bimetallic catalysts such as Rh–Co [1,2,12,37,38], Rh–Fe [11,12,14,17,22,23], Rh–Ag [29], Rh–Mo [24]. The reduction of transition metal salts in aqueous solution with $NaBH_4$ is known to cause the formation of nanocrystalline or amorphous metallic phases [41]. The formation of amorphous borides was observed when nickel and cobalt salts were reduced by this method [42,43].

* Corresponding author. Tel.: +39-41-5298562; fax: +39-41-5298517.

PII S1381-1169(96)00243-9

In spite of the extensive use, the chemistry of the process is still not well understood. Nevertheless, in the case of Ni, Co, Cu and Fe, the experimental conditions to, respectively, produce a metal boride or a nanocrystalline metallic powder have been recently described in detail [43].

We have recently described highly chemoselective Rh/B and Rh/Al vapor phase hydroformylation catalysts prepared by low temperature reduction of rhodium salts, adsorbed on silica and silica alumina, with $NaBH_4$ and $LiAlH_4$ [34–36], respectively. It was observed that oxidized boron and aluminum particles played an important role in protecting the metallic catalyst from sintering and preventing H_2 dissociation with a substantial reduction of the olefin hydrogenation activity. An increased chemoselectivity towards hydroformylation was therefore observed.

Supported catalysts based on the Rh–Co couple, mainly derived from the decomposition of bimetallic carbonylic clusters, were found particularly active and selective in the vapor phase hydroformylation of simple olefins provided that the two metals were in intimate contact [1,2,12,37,38].

Here we report the preparation, characterization and reactivity studies on propene hydroformylation of Rh–Co based catalysts, with various Rh/Co ratios, obtained by the reduction of the metal salts coadsorbed on silica with $NaBH_4$ in anaerobic conditions.

2. Experimentals

2.1. Materials

Silica was a Grace 432(3) silica catalyst support with a surface area of 320 $m^2\ g^{-1}$, pore volume of 1.2 ml g^{-1}, and particle size of 30–100 μm. $RhCl_3 \times 3H_2O$ was used as received from Janssen Chimica. All gases (SIAD 99.9%) were used without further purification.

2.2. Catalyst preparation

2.2.1. Preparation of $Rh_{50}Co_{50}/SiO_2$

$CoCl_2 * 6H_2O$ (1.0 mmol) and $RhCl_3 * 3H_2O$ (1.0 mmol) dissolved in distilled water (10 ml) were slowly added to silica (5 g) suspended in water (100 ml). The mixture was maintained at 338 K under constant stirring for 2 h and then the solvent was removed under reduced pressure with a rotavapor.

The resultant powder was rapidly added under argon to an ice (273 K) cooled solution of $NaBH_4$ (1 g) in 500 ml of deaerated distilled water. An immediate effervescence was observed and a black powder slowly settled. The catalyst was filtered under Ar, washed many times with deaerated distilled water and dried under vacuum.

All the other samples with different Rh/Co atomic ratios were prepared following the procedure described above.

2.3. Characterization methods

2.3.1. X-ray diffraction

The samples were examined in the θ–2θ reflection geometry with a Philips PW 1310 powder diffractometer working at 45 kV and 25 mA. The beam emitted by a Cu anode was collimated with 1/2° divergence slit. The diffracted ray was scanned with a 0.2 mm slit and focused to the counter with a graphite monochromator. The surface area was calculated from the X-ray diffraction of the surface weighted crystallite mean obtainable from the Fourier coefficients of deconvoluted peak profiles.

2.3.2. XPS analysis

XPS spectra were run on a Vacuum Generators ESCALAB spectrometer, equipped with a hemispherical analyzer operating in the fixed analyzer transmission (FAT) mode, with a pass energy of 20 or 50 eV. Al k$\alpha_{1,2}$ and Mg k$\alpha_{1,2}$ photons ($h\nu$ = 1486.6, 1253.6 eV, respectively)

were used to excite photoemission. All samples were measured as powders pressed on a metal tip or spread on double-side scotch tape. The binding energy (BE) scale (eV) was calibrated by taking the Au $4f_{7/2}$ peak at 84.0 eV. Correction of the energy shift due to the static charging of the samples was accomplished using as reference the Si 2p peak from the support taken at 103.6 eV. The accuracy of the reported binding energies (BEs) was ± 0.2 eV, and the reproducibility of the results was within these values. The spectra were collected by a DEC PDP 11/83 data system and processed by means of VGS 5200 data handling software.

2.3.3. FT-IR spectroscopy

The IR spectra were recorded on a Nicolet Magna 750 interferometer at a resolution of 4 cm^{-1}. To simulate the reactor environment, the adsorption of the CO, CO/H_2 (1:1) and hydroformylation mixture, was studied in an evacuable IR pyrex cell with CaF_2 windows. The catalysts were ground to a fine powder, pressed into self-supporting wafers at a pressure of ca. 6 MPa and mounted in the holder of the IR cell. All the measurements were carried out at 0.101 MPa.

2.3.4. Temperature-programmed reduction

Temperature programmed reduction (TPR) was performed in a conventional, U-shaped, quartz microreactor ($\varnothing = 6$ mm, $l = 200$ mm) using a 5% H_2 in Argon mixture flowing at 35 ml min^{-1} (STP). TPR measurements were taken between 295 and 900 K with a heating rate of 10 K min^{-1}. The reduction of CuO to metallic copper was used to calibrate the TPR apparatus for H_2 consumption.

2.3.5. Catalytic measurements

The hydroformylation of propene was carried out in a tubular stainless-steel flow reactor, with a flow system at atmospheric pressure. Gas chromatographic analysis was achieved by using two gas chromatographs. The gas chromatograph A was used to separate and analyze the aldehydes with a 25 m fused silica Poraplot Q ($\varnothing = 0.53$ mm) column while gaschromatograph B was used to separate hydrocarbons with a Plot fused silica Al_2O_3/KCl 25 m column ($\varnothing = 0.53$ mm).

The catalysts were treated in an argon flow at 543 K for 24 h and in a $CO/H_2 = 1$ flow (20 ml min^{-1}) at 453 K for 24 h.

Pressure was controlled by means of a relief valve, using N_2 as a reference, gas counteracting on a PTFE membrane.

The typical hydroformylation conditions were: 1/1/1/15 mixture of CO/H_2/propene/N_2 flowing at 27 ml min^{-1}, space velocity 3100 h^{-1}.

3. Results

3.1. X-ray diffraction

The X-ray diffraction spectra of the 'as prepared' Rh–Co/B samples showed only signals attributable to metallic rhodium fcc (face centered cubic) crystallites with diameter of ca. 2.5 nm. Some representative spectra are shown in Fig. 1.

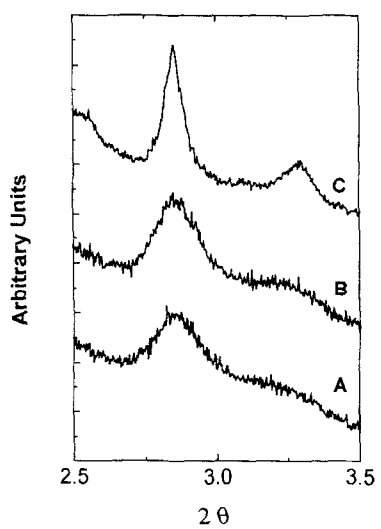

Fig. 1. XRD pattern of: (A) Rh_{50}–Co_{50}–B/SiO_2; (B) Rh_{50}–Co_{50}–B/SiO_2 treated in CO/H_2 at 473 K; (C) Rh_{50}–Co_{50}–B/SiO_2 treated in air at 723 K and in hydrogen at 623 K.

No modifications were found in the XRD spectrum (A) of the sample prepared under anaerobic conditions, even after treatment in CO/H_2 at 473 K (B). Oxidation of the Rh–Co/B samples in air at 723 K followed by reduction in hydrogen at 623 K resulted in an increase of the rhodium crystallites dimensions up to 4 nm in diameter. Metallic cobalt was never detected by XRD.

3.2. X-ray photoelectron spectroscopy measurements

The data of the related Rh–Co/B and Rh/B [34] systems on silica are summarized in Table 1.

The Co/Rh atomic ratios were calculated from the Co $2p_{3/2}$/Rh $3d_{5/2}$ area ratios. The spectra were recorded soon after sample preparation and air exposure was avoided, though not all the operations were conducted in an inert atmosphere.

The spectra of the Rh–Co/B samples in the Rh $3d_{5/2}$ and Co $2p_{3/2}$ core levels presented a signal at 307.7 ± 0.2 eV attributable to reduced Rh and a signal at 781.5 ± 0.2 eV with a satellite at 787.0 eV typical of Co^{2+} probably Co oxide/hydroxide [44].

The Co/Rh atomic ratios values evidenced a strong Co enrichment of the surface even in the rhodium rich Rh_{75}–Co_{25}/B sample where the molar ratio of the starting materials was Rh/Co = 3.

The spectrum of Rh/B, already reported in a previous paper [34], showed two Rh $3d_{5/2}$ components at 307.5 ± 0.2 and 309.2 ± 0.2 eV, respectively. The first signal at 307.5 ± 0.2 eV could be assigned to zerovalent rhodium and the second at 309.5 ± 0.2 eV to an oxidized rhodium species.

The spectrum of Co/B showed two Co $2p_{3/2}$ components at 778.0 ± 0.2 and 781.5 ± 0.2 eV, respectively. The cobalt signal at 778.0 ± 0.2 eV was clearly due to zerovalent Co while the signal at 781.5 ± 0.2 eV was attributed to Co oxide/hydroxide.

No significative boron amounts were detected in the Co/B and Rh–Co/B samples, while significant boron signals were recorded for Rh/B [34].

3.3. Temperature-programmed reduction analysis

Temperature-programmed reduction (TPR) and temperature-programmed oxidation (TPO) have been largely used to study supported mono and bimetallic catalysts [45,46].

The most important question that has to be answered in the case of supported bimetallic catalysts is whether the surface particles really contain atoms of both metals.

Table 1
Binding energies (eV) [a] and XPS atomic ratios for reported compounds

Sample	Co $2p_{3/2}$ ox	Co $2p_{3/2}$ red	Rh $3d_{5/2}$ ox.	Rh $3d_{5/2}$ red.	M_{ox}/M_{red}	B_{Tot}/Rh_{Tot}	Co_{Tot}/Rh_{Tot}
$Rh-B/SiO_2$ [b]			309.2	307.5	2.0	1.9	
$Rh_{75}-Co_{25}-B/SiO_2$	781.4			307.7		n.d.	1.1
Satellite	786.3						
$Rh_{50}-Co_{50}-B/SiO_2$	781.7			307.5		n.d.	4.2
Satellite	787.6						
$Rh_{25}-Co_{75}-B/SiO_2$	781.6			307.3		n.d.	6.9
Satellite	786.5						
$Co-B/SiO_2$	781.5	778.0			7.2		
Satellite	786.0						

[a] All binding energies (BEs) were calibrated by taking the Si 2p at 103.6 eV. The accuracy of the reported BE is 0.2 eV and the reproducibility of the results was within these values.
bRef. [34].

The TPR technique can be used to obtain evidence of the interaction between the atoms of the two metallic components, identifying alloyed phases or intimate contact between the two partners.

The Rh–Co system supported on alumina, titania and silica [47,48] was studied by TPR and TPO and the results were correlated with the XRD and EXAFS data.

It was reported [48] that the reduction of a Co/SiO_2 sample, prepared by conventional impregnation of the chloride started at 473 K and was complete at 973 K. The reduction of the analogously prepared Rh/SiO_2 was complete at 473 K. Two peaks were visible in the rhodium TPR profiles, at 368 K and at 413 K, respectively, assignable to Rh oxide and rhodium chloride reduction [48].

The TPR profile of the silica supported bimetallic Co and Rh catalysts showed that the reduction took mainly place between 273 and 510 K. This demonstrated that the rate of reduction of the cobalt salt was enhanced by the presence of rhodium, suggesting that the two metals were in intimate contact within each other [48].

EXAFS of the Rh K-edge of the Co–Rh/SiO_2 confirmed that, as was already suggested by TPR results, the reduced catalyst contained bimetallic Co–Rh particles, the interiors of which were enriched in rhodium, while the outer layer contained more cobalt [48].

We studied the TPR behavior of the as prepared Rh/B and Rh–Co/B samples.

In Fig. 2, we report the TPR profiles in the 300–900 K temperature range, of Rh/B and of two selected Rh–Co/B samples, both as prepared and after oxidation in air at 723 K.

The Rh/B TPR profile (curve A) presented a reduction peak at 380 K attributable to the reduction of the small amount of oxidized surface rhodium also detected by XP-spectroscopy [34].

The TPR profile of the Rh/B sample after air oxidation (curve B) showed the characteristic reduction pattern of silica supported Rh_2O_3;

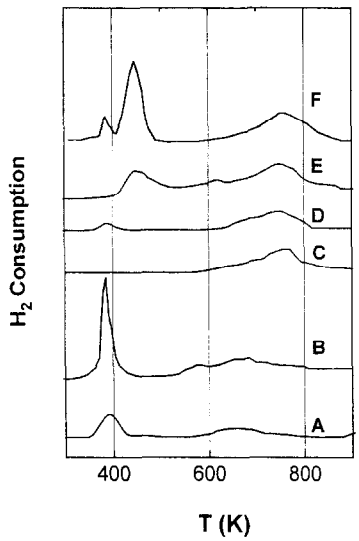

Fig. 2. TPR profiles of SiO_2 supported Rh/B and Rh–Co/B systems in the 300–900 K range: (A) $Rh–B/SiO_2$ as prepared; (B) $Rh–B/SiO_2$ after air oxidation at 723 K; (C) $Co–B/SiO_2$ as prepared; (D) $Rh_{50}–Co_{50}–B/SiO_2$ as prepared; (E) $Rh_{50}–Co_{50}–B/SiO_2$ after air oxidation at 723 K; (F) $Rh_{75}–Co_{25}–B/SiO_2$ after air oxidation at 723 K.

the reduction was complete at 420 K with a maximum at 386 K.

The curve of the as prepared Co/B sample showed a single broad reduction peak centered at 765 K (curve C). The curve profile of the oxidized sample resulted identical for both peak position and intensity, indicating that most of the cobalt was not reduced by $NaBH_4$ as also indicated by the BEs values found.

The TPR profile (curve D) of the as prepared $Rh_{50}–Co_{50}/B$ sample (the behavior of $Rh_{25}–Co_{75}/B$ was very similar) showed the reduction peak of cobalt in the 730–900 K temperature range, while only an extremely weak peak was present in the 'Rh reduction range', confirming what detected by XPS. Some oxidized rhodium was probably formed during sample handling in air before the TPR experiments.

Both the Rh–Co/B samples presented, after oxidation, a reduction band centered at 450 K which was complete at 500 K and a Co reduction band centered at 765 K.

The reduction bands in the 'cobalt region' of the TPR profiles of all Rh–Co/B catalysts hav-

ing the same intensities in both as prepared and oxidized samples further confirmed that the cobalt was not reduced by $NaBH_4$ in the bimetallic samples, as well as was found by XP-spectroscopy.

The rhodium reduction peak of the oxidized samples shifted to higher temperatures (450–500 K), suggested a close interaction between the cobalt and rhodium oxides, if not the formation of a mixed oxide.

The TPR profile of the oxidized Rh_{75}–Co_{25}/B sample (curve F) showed two reduction peaks in the rhodium reduction region, respectively at 386 and 450 K which might indicate that part of the rhodium was segregated and present on the surface as monometallic particles.

3.4. IR spectra

The IR spectra of the samples of Rh/B and Rh–Co/B exposed to a CO flow in an evacuable cell at room temperature were recorded in order to study the exposed metal sites in the as prepared samples.

The IR spectrum of Rh/B catalyst, after exposition to CO flow at 298 K for 48 h, was already reported by us [34] and showed two twin bands at 2015 and 2088 cm^{-1} in the $\nu_{(CO)}$ region attributed to the stretching vibrational modes of two carbonyl groups coordinated to a Rh(I) center bonded to the oxide surface (Fig. 3, spectrum D). Treatment in CO/H_2 at temperatures up to 453 K resulted in the appearance of two broad bands, respectively at 2015 cm^{-1} (with a shoulder at 2040 cm^{-1}) and 1850 cm^{-1} together with a considerable decrease of the bands intensity (Fig. 3, spectrum E). The shoulder could be due to the stretching vibration of the linearly coordinated CO on reduced rhodium sites or to the C–O stretching mode of a 'rhodium carbonyl hydride species' [49,50]. The band at 2015 cm^{-1} was thought attributable either to a chlorine containing carbonyl or to an adsorption with a significant contribution from a

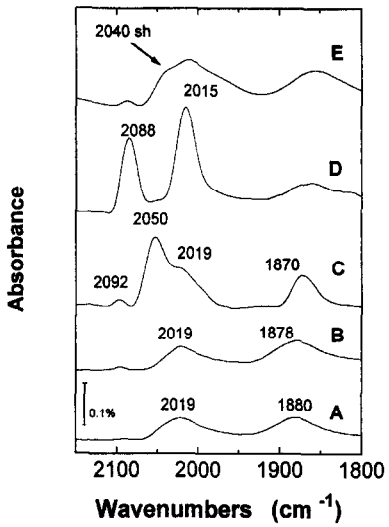

Fig. 3. FT-IR spectra in the $\nu_{(CO)}$ region: (A) Rh_{50}–Co_{50}–B/SiO_2 as prepared after exposure to CO at 298 K for 48 h; (B) Rh_{50}–Co_{50}–B/SiO_2 after exposure to CO/H_2 at 453 K for 24 h; (C) Rh_{75}–Co_{25}–B/SiO_2 as prepared after exposure to CO at 298 K for 48 h; (D) Rh–B/SiO_2 as prepared after exposure to CO at 298 K for 48 h; (E) Rh–B/SiO_2 as prepared after exposure to CO/H_2 at 453 K for 24 h.

bridge-bonded CO [35]. The presence of chlorine atoms was proved by XPS.

On the other hand, the IR spectrum (Fig. 3, spectrum A) of the Rh_{50}–Co_{50}/B sample exposed at 298 K to flowing CO presented two weak bands at 2019 and 1880 cm^{-1}, respectively, typical of CO linearly and bridged bonded to metallic rhodium sites. Thermal treatment in CO/H_2 at temperatures up to 453 K produced only little variations of the bands frequencies and intensities (Fig. 3, spectrum B).

The band at 2019 cm^{-1} can be analogously attributed to the bands at 2015 cm^{-1} of Rh/B [34,35] or Rh/Al [36]. The entire spectrum was in any case less intense than that of Rh/B and the intensity of the bands was dependent on the rhodium content.

The IR spectrum of Rh_{75}–Co_{25}/B after exposure to CO at 298 K for 48 h (Fig. 3, spectrum C) showed the coexistence of various species on the catalyst surface. The spectrum was interpreted attributing the features at 1870 and 2019 cm^{-1} to the Rh–Co/B system while the bands at 2050, 2092 and part of the band at

2019 cm^{-1} appeared to belong to a monometallic Rh system probably similar to Rh/B [34]. Part of the 2019 cm^{-1} band most likely belongs to the twin bands system (2092 and 2019 cm^{-1}) characteristic of the Rh(I) gem-coordinated carbonyls.

3.5. Catalytic tests

All the prepared samples, pretreated in CO/H_2 at 453 K for 24 h before the reaction, were tested in the vapor phase propene hydroformylation.

We have previously reported the results of the vapor phase hydroformylation of ethylene and propene on the Rh/B system catalysts at atmospheric pressure [34,35].

All the Rh–Co/B systems resulted totally inactive in the same experimental conditions, with the only exception of Rh_{75}–Co_{25}–B/SiO_2 that showed a negligible hydroformylation activity at 453 K, probably due to the small amount of Rh/B species present.

The other Rh–Co/B catalysts were active only at pressures above 506 kPa. However the Rh–Co/B catalysts showed high values of both chemo- and regio-selectivities.

The chemoselectivity towards hydroformylation (R) decreased with the increasing temperature while the regioselectivity to the linear hydroformylation products (S_L) was almost invariant for both catalysts with the changing reaction temperature.

4. Discussion

Bimetallic systems, constituted by highly dispersed entities of two different metals, represent an important class of heterogeneous catalysts [51–54]. It can be reasonably supposed that metal couples which in the bulk solid solutions easily form alloy clusters when reduced on the surface of the support. The closely interacting alloyed metallic species can mutually modify their chemical and structural properties. These modifications are experimentally well established, but theoretically still not fully understood [55].

Moreover, it is sometimes very difficult to determine if the surface particles are authentically bimetallic and, in that case, their exact morphology.

The reduction of two salts co-adsorbed on an inorganic support is widely used to obtain supported bimetallic particles. It was claimed that reduction with aqueous alkaly borohydride of mixed aqueous solutions of iron and cobalt salts gave origin to ultra-fine amorphous Fe–Co alloy particles [56]. Nevertheless, it was recently reported that anaerobic sodioborohydride reduction of cobalt chloride in water produced only cobalt boride Co_2B [43]. The metal reoxidation is even easier when the metal salt is supported on an oxide [12]. On the other hand it clearly resulted, from our XPS and TPR data, that $CoCl_2$ adsorbed on silica treated with aqueous $NaBH_4$ at 273 K in anaerobic conditions neither formed borides nor metallic cobalt.

The same can be said for the cobalt contained in the Rh–Co/B catalysts. Moreover, a remarkable superficial cobalt enrichment was observed by XPS in all the Rh–Co samples.

A shift to higher temperatures of the rhodium reduction peak was observed in the TPR profile of all the bimetallic samples analyzed after air oxidation at 723 K. This behavior was generally taken as an indication of an intimate contact between the two metallic species [45,46]. It is reasonable to presume that also the as prepared catalyst samples were formed by bimetallic particles.

The TPR peak in the 'rhodium reduction region' shifted to higher temperatures can in fact be attributed to the reduction of closely interacting cobalt and rhodium oxides, if not to the reducing process of a mixed oxide $RhCoO_x$. It was also observed that part of the cobalt was still reduced in the normal cobalt reduction temperature range.

The TPR curve profile of the sample Rh_{75}–

Co_{25}–B/SiO_2, showed two reduction bands in the Rh reduction range. This finding can be explained by assuming that in this case small monometallic rhodium crystallites, similar to Rh–B coexist with the bimetallic Rh–Co particles on the silica surface.

It can be proposed from these data that the bimetallic catalysts obtained by the reduction of the coadsorbed Co and Rh salts are most probably constituted by rhodium particles covered in part by a cobalt oxide layer.

Also, FT-IR, XPS and reactivity data can find their rationale within this model. Unfortunately, information obtained from FT-IR spectra of adsorbed CO were very limited because it was not technically possible to study the system at the reaction operating pressure.

The two weak carbonylic bands observed after atmospheric pressure CO adsorption (Fig. 3, curve A) can indicate that only few rhodium surface sites are available to chemisorb the CO molecules. The spectrum (Fig. 3, spectrum B) was not modified after exposure to CO/H_2 at 453 K, while surface disruption–reconstruction phenomena were always observed on similar supported rhodium samples after thermal treatments in CO/H_2 [34,36].

All the catalysts were found totally inactive in the hydroformylation of propene at atmospheric pressure, even after a complete oxidation (in air) and reduction (in H_2) cycle. Nevertheless, when the system was slightly pressurized (506 kPa) acceptable hydroformylation activity and excellent selectivity were observed.

Comparison with XPS and FT-IR data of the related Rh/B [34,35] and Rh/Al [36] systems

Table 2
Product distribution for propene hydroformylation catalyzed by SiO_2 supported Rh/B and Rh–Co/B systems at 506 kPa

	T (K)	r (propane) [a]	r (*n*-butanal) [a]	r (*iso*-butanal) [a]	S_L [b]	R [c]
Rh–B/SiO_2	403	0.36	0.55	0.18	75	0.67
	423	1.10	0.99	0.35	74	0.55
	453	4.50	1.76	0.66	73	0.35
	473	10.57	2.48	0.90	73	0.24
	493	29.6	3.52	1.30	73	0.14
	E_a (kJ mol^{-1})	75.0	32.0			
Rh_{75}–Co_{25}/SiO_2	403	1.10	2.84	0.33	89	0.74
	423	3.76	3.93	0.54	88	0.54
	453	13.56	6.67	0.82	89	0.36
	473	28.44	8.65	1.07	89	0.25
	493	91.31	15.00	2.05	88	0.16
	E_a (kJ mol^{-1})	74.0	32.7			
Rh_{50}–Co_{50}/SiO_2	403	0.52	1.39	0.06	96	0.74
	423	1.77	2.29	0.10	96	0.57
	453	6.07	3.96	0.30	93	0.41
	473	10.55	6.00	0.69	90	0.38
	493	40.00	9.90	1.26	89	0.22
	E_a (kJ mol^{-1})	71.8	35.0			
Rh_{25}–Co_{75}/Sio_2	403	0.04	0.10	n.d.		0.71
	423	0.11	0.14	n.d.		0.56
	453	0.37	0.25	0.01	96	0.41
	473	0.88	0.50	0.03	94	0.38
	493	2.27	0.61	0.07	90	0.23
	E_a (kJ mol^{-1})	74.0	34.7			

[a] r = mol g_{Rh}^{-1} h^{-1} 10^3.
[b] S_L = (*n*-isomer/total hydroformylation products) × 100 ratio.
[c] R = hydroformylation/propene consumption ratio.

can give some help in understanding the catalytic behavior of the Rh–Co/B system.

The Rh $3d_{5/2}$ BE values are very similar in the three systems and are attributable to Rh(0) species even if XP-spectroscopy is scarcely sensitive to light variations of the oxidation state.

The catalytic behavior of the Rh/B system at atmospheric pressure was already described by us [35]. The catalysts tested at 506 and 1013 kPa (Tables 2 and 3) showed, in comparison with the reaction at atmospheric pressure, a regioselectivity decrease and a slight increase of chemoselectivity values. On the other hand, the Rh–Co/B catalysts were found totally inactive at atmospheric pressure while at 506 and 1013 kPa they actively and selectively catalyzed the reaction, with peak S_L and R values of 96 and 0.75, respectively. A close inspection of the reactivity data showed that the apparent activation energy (E_a) for the atmospheric hydroformylation reaction catalyzed by Rh/B was 42 kJ mol^{-1} while Rh/B and Rh–Co/B catalyzed the reaction at 506 and 1013 kPa, respectively, with an activation energy of 32 and 35 kJ mol^{-1}. The previously described Rh/Al system [36] catalyzed the reaction at 0.1 MPa with an $E_a = 21$ kJ mol^{-1}. These data suggested that the atmospheric reaction on Rh/B occurred most probably on sites different from those of the pressurized system. In the light of these findings it can be useful to compare the IR spectra of Rh/B, Rh/Al and Rh–Co/B, respectively, revisiting the attribution of the 2019 cm^{-1} band of Rh–Co/B. A band in the 2015–2020 cm^{-1}

Table 3
Product distribution for propene hydroformylation catalyzed by SiO_2 supported Rh/B and Rh–Co/B systems at 1013 kPa

	T (K)	r (propane) [a]	r (n-butanal) [a]	r (*iso*-butanal) [a]	S_L [b]	R [c]
$Rh-B/SiO_2$	403	0.63	0.98	0.3	74	0.68
	423	1.9	1.34	0.52	72	0.49
	453	6.94	1.97	0.77	72	0.28
	473	18	2.7	1.05	72	0.17
	493	49.7	3.55	1.32	73	0.09
	E_a (kJ mol^{-1})	75.0	31.5			
$Rh_{75}-Co_{25}/SiO_2$	403	1.55	4.05	0.45	90	0.74
	423	5.54	6.8	0.94	89	0.58
	453	20.39	13.17	1.55	89	0.42
	473	54.85	20.05	2.48	89	0.29
	493	163.71	29	3.95	88	0.17
	E_a (kJ mol^{-1})	74.0	36.4			
$Rh_{50}-Co_{50}/SiO_2$	403	0.63	1.78	0.09	95	0.75
	423	1.85	2.97	0.16	95	0.63
	453	6.94	5.68	0.49	92	0.47
	473	15.7	8.51	0.88	90	0.37
	493	50.0	11.7	1.34	90	0.21
	E_a (kJ mol^{-1})	74.0	34.7			
$Rh_{25}-Co_{75}/SiO_2$	403	0.07	0.15	n.d.		0.68
	423	0.18	0.26	n.d.		0.59
	453	0.87	0.5	0.02	96	0.37
	473	1.82	0.64	0.06	91	0.28
	493	5.76	0.91	0.09	91	0.15
	E_a (kJ mol^{-1})	74.0	33.7			

[a] r = mol g_{Rh}^{-1} h^{-1} 10^3.
[b] S_L = (n-isomer/total hydroformylation products) × 100 ratio.
[c] R = hydroformylation/propene consumption ratio.

region was found in all three catalysts after treatment in CO/H_2. Nevertheless only the metal carbonyl band at 2015 cm^{-1} of Rh/Al appeared attributable to a species involved in the catalytic process at atmospheric pressure [36]. The corresponding bands detected in the other two systems appeared to belong to species not involved in the catalytic process. This can indicate that those species are quite similar between themselves but different from those detected on Rh/Al. We are nevertheless very far from a satisfactory attribution of these IR adsorptions to well defined surface species.

The catalytic properties of the Rh–Co/B system can be summarized as follows:

(a) specific activity calculated relative to rhodium weight increase with the Rh/Co ratio;

(b) chemoselectivity towards hydroformylation was comparable with that of Rh/B;

(c) selectivity to linear hydroformylation products was very high (in some cases the highest value ever found to our knowledge for propene hydroformylation in vapor phase on rhodium supported catalysts).

The attribution of this behavior to the surface coverage by cobalt oxide can only be tentative, because of the complete lack of spectroscopic data at higher than atmospheric pressure.

It is well known that olefin hydrogenation successfully competes with heterogeneous hydroformylation on rhodium at atmospheric pressure [3,4,6].

It was demonstrated that the addition of suitable promoters to rhodium lead to a remarkable improvement of the chemoselectivity values [12–14,16–18,22–31,34–40].

The promoters can operate in various and sometimes multiple ways according to their nature. Some dopants or promoters appeared to mainly act by blocking the multicenter rhodium sites where the CO and H_2 dissociation which require large sites occurs. A remarkable suppression of olefin hydrogenation that can favorably compete with hydroformylation on such kinds of sites was therefore obtained [10,11,13,26]. It was proposed that hydroformylation requires only small rhodium ensembles and selectively occurs on protruding edge and corner sites of the rhodium crystallite. A catalyst formed by small metal crystallites with a larger number of edges and corners per weight unit should be more selective for the hydroformylation. The relationship between the dimensions of metal crystallites (or catalyst dispersion) with the activity and selectivity was underlined in various studies [13,15,38,40].

The most surprising property of our Rh–Co catalyst is their total inertness towards both hydrogenation and hydroformylation at atmospheric pressure and their good performance as soon as a weak pressure was applied.

In the absence of more detailed information the previously sketched model with particles composed of a metallic rhodium core almost completely covered by a layer of cobalt oxide can offer a qualitative explanation. The model is similar to that used to explain the catalytic behavior of the supported Cu–Ru immiscible couple [50–52]. When supported rhodium catalysts are sulfidated or treated with zinc ions [10,11,13,18,19] the dopant atoms are preferentially chemisorbed on the flat or hollow sites of the crystallites while protruding edge and corner atoms are not affected.

In our probably oversimplified model, cobalt oxide appears to cover, with a thick poliatomic and irregular layer, almost all the rhodium surface leaving only few narrow windows available for the chemisorption of the incoming reacting molecules. The chemisorption of the small CO molecule was observed by FT-IR but the coadsorption of the other reactants necessary for the reaction to occur is probably severely physically hindered at atmospheric pressure. The pressure is probably necessary to force the reactants molecules (CO, H_2, C_2H_6) onto the relatively inaccessible catalytic sites. The constrained environment of the active sites probably hinders the formation of the bulkier branched isomer giving an explanation of the high value of the selectivity of these catalysts towards linear products.

Acknowledgements

The financial support of M.U.R.S.T. (Ministero dell'Università e Ricerca Scientifica) and of the C.N.R (Consiglio Nazionale delle Ricerche) – Progetto Strategico "Tecnologie Chimiche Innovative" is acknowledged. The authors thank A. Talon for the analytical determinations.

References

[1] M. Ichikawa, J. Catal. 56 (1979) 127.
[2] M. Ichikawa, J. Catal. 59 (1979) 67.
[3] H. Arai and H. Tominaga, J. Catal. 75 (1982) 188.
[4] N. Takahashi, S. Hasegawa, N. Hanada and M. Kobayashi, Chem. Lett. (1983) 945.
[5] N. Takahashi, H. Matsuo and M. Kobayashi, J. Chem. Soc., Faraday Trans. I 80 (1984) 629.
[6] N. Takahashi and M. Kobayashi, J. Catal. 85 (1984) 89.
[7] M.E. Davis, E. Rode, D. Taylor and B.E. Hanson, J. Catal. 86 (1984) 67.
[8] E. Rode, M.E. Davis and B.E. Hanson, J. Catal. 96 (1985) 563.
[9] E. Rode, M.E. Davis and B.E. Hanson, J. Catal. 96 (1985) 574.
[10] M. Ichikawa, A.J. Lang, D.F. Shriver and W.M.H. Sachtler, J. Am. Chem. Soc. 107 (1985) 7216.
[11] W.M.H. Sachtler and M. Ichikawa, J. Phys. Chem. 90 (1986) 4752.
[12] M. Ichikawa, Homogeneous and Heterogeneous Catalysis, Yu.I. Yermakov and V.A. Likhobolov (Eds.) (VNU Science Press, Utrecht, 1986).
[13] Y. Konishi, M. Ichikawa and W.M.H. Sachtler, J. Phys. Chem. 91 (1987) 6286.
[14] A. Fukuoka, M. Ichikawa, J.A. Hriljac and D.F. Shriver, Inorg. Chem. 26 (1987) 3645.
[15] H. Arakawa, N. Takahashi, T. Hanaoka, K. Takeuchi, T. Matsukaki and Y. Sugi, Chem. Lett. (1988) 1917.
[16] Y. Izumi, K. Asakura and Y. Iwasawa, J. Chem. Soc., Chem. Commun. (1988) 1286.
[17] M. Ichikawa, Polyhedron 7 (1988) 2351.
[18] S.S.C. Chuang and S.-I. Pien, J. Mol. Cat. 55 (1989) 12.
[19] S. Naito and M. Tanimoto, J. Chem. Soc., Chem. Commun. (1989) 1403.
[20] N. Takahashi, A. Mijin, H. Suematsu, S. Shinoara and H. Matsuoka, J. Catal. 117 (1989) 348.
[21] A. Fukuoka, L. Rao, N. Kosugy, H. Kuroda and M. Ichikawa, Appl. Catal. 50 (1989) 295.
[22] A. Fukuoka, T. Kimura, N. Kosugi, H. Kuroda, Y. Minai, Y. Sakai, T. Tominaga and M. Ichikawa, J. Catal. 126 (1990) 434.
[23] M. Ichikawa, L. Rao, T. Kimura and A. Fukuoka, J. Mol. Catal. 15 (1990) 62.
[24] A. Trunschke, H. Ewald, H. Miessner, A. Fukuoka, M. Ichikawa and H.C. Boettcher, Mater. Chem. Phys. 29 (1991) 503.
[25] S. Naito and M. Tanimoto, J. Catal. 130 (1991) 106.
[26] M.W. Balakos, S.I. Pien and S.S.C. Chuang, Stud. Surf. Sci. Catal. 68 (1991) 549.
[27] Y. Izumi, K. Asakura and Y. Iwasawa, J. Catal. 127 (1991) 631
[28] Y. Izumi, K. Asakura and Y. Iwasawa, J. Catal. 132 (1991) 566.
[29] S.S.C. Chuang and S.I. Pien, J. Catal. 135 (1992) 618.
[30] S.S.C. Chuang and S.I. Pien, J. Catal. 138 (1992) 536.
[31] G. Srinivas, S.S.C. Chuang, J. Catal. 144 (1993) 131.
[32] S.S.C. Chuang, G. Srinivas and A. Mukherjee, J. Catal. 139 (1993) 490.
[33] M. Lenarda, R. Ganzerla, L. Storaro, A. Trovarelli, R. Zanoni and J. Kaspar, J. Mol. Catal. 72 (1992) 75.
[34] M. Lenarda, R. Ganzerla, L. Storaro and R. Zanoni, J. Mol. Catal. 78 (1993) 339.
[35] M. Lenarda, R. Ganzerla, L. Storaro and R. Zanoni, J. Mol. Catal. 79 (1993) 243.
[36] M. Lenarda, R. Ganzerla, S. Enzo, L. Storaro and R. Zanoni, J. Mol. Catal. 80 (1993) 105.
[37] L. Huang, Y. Xu, G. Piao, A. Liu and W. Zhang, Catal. Lett. 23 (1994) 87.
[38] L. Huang, Y. Xu, W. Guo, D. Li and X. Guo, Catal. Lett. 32 (1995) 61.
[39] A. Fusi, R. Psaro, C. Dossi, L. Garlaschelli and F. Cozzi, J. Mol. Catal. (1995), in press.
[40] L. Sordelli, R. Psaro, C. Dossi and A. Fusi, Catalysis and Surface Characterization, T.J. Dines, C.H. Rochester and J. Thompson (Eds.) (The Royal Society of Chemistry, Cambridge, 1992) p. 127.
[41] R.C. Wade, in: Speciality Inorganic Chemicals, R. Thompson (Ed.) (The Royal Soc., London, 1981) p. 25; H.C. Brown and C.A. Brown, J. Am. Chem. Soc. 84 (1962) 1493, 2827.
[42] A. Corrias, G. Ennas, G. Licheri, G. Marongiu and G. Paschina, Chem. Mater. 2 (1990) 363; G. Carturan, S. Enzo, R. Ganzerla, M. Lenarda and R. Zanoni, J. Chem. Soc., Faraday Trans. 86 (1990) 739; A. Corrias, G. Ennas, A. Musinu, G. Marongiu and G. Paschina, Chem. Mater. 5 (1993) 1722.
[43] G.N. Glavee, K.J. Klabunde, C.M. Sorensen and G.C. Hadjipanayis, Langmuir 9 (1993) 162; 10 (1994) 4726.
[44] D. Briggs and M.P. Seah, Practical Surface Analysis by Auger and X-Ray Photoelectron Spectroscopy, Vol. 1, 2nd Ed. (J. Wiley and Sons, Chichester, 1990).
[45] N.W. Hurst, S.J. Gentry, A. Jones and B.D. Mc Nicol, Catal. Rev. Sci. Eng. 24 (1982) 233.
[46] A. Jones and B.D. Mc Nicol, Temperature Programmed Reduction for Solid Materials Characterization (Marcel Dekker, N.Y., 1986).
[47] H.F.J. van 't Blink, D.C. Koningsberger and R. Prins, J. Catal. 97 (1986) 188, 200.
[48] H.F.J. van 't Blink, D.C. Koningsberger and R. Prins, J. Catal. 97 (1986) 210.
[49] F. Solymosi, A. Erdohelyi and M. Kocsis, J. Catal. 65 (1980) 428; F. Solymosi and A. Erdohelyi, J. Catal. 70 (1981) 451.

[50] J.H. Sinfelt, J. Catal. 29 (1973) 308.
[51] J.H. Sinfelt, Acc. Chem. Res. 10 (1977) 15.
[52] J.H. Sinfelt, Rev. Mod. Phys. 51 (1979) 569.
[53] J.K.A. Clarke, Chem. Rev. 75 (1975) 291.
[54] J.K.A. Clarke, A.C.M. Creaner, Ind. Eng. Chem. Prod. Res. Dev. 20 (1981) 574.
[55] F.J.C.M. Toolenar, F. Stoop and V. Ponec, J. Catal. 82 (1983) 1.
[56] J. van Wonterghem, S. Mørup, C.J. Koch, S.W. Charles and S. Wells, Nature 322 (1986) 622.